Evaluation of the Instrumented Indentation as a Tool to Estimate the Mechanical Properties for Engineering Materials

[*]Eng.Ahmed. F. Elmisteri [*]Dr. Abdelbaset R.H. Midawi [*] Pro.Farag M Shuaeib

Abstract: Instrumented indentation technique at micro-scales has become more popular to determine mechanical properties of materials like hardness, modulus of elasticity, and yield strength. It is introduced as a method that finds the stress-strain curve, instead of traditional tensile test. Whereas it gives possibility to determine the mechanical properties for small specimens, and material under operation in the field. Several researchers have attempted to evaluate this method experimentally and to investigate the factors effecting it by using different shape of indenters, and different types of materials. In the same regard, this research work is conducted to evaluate this method experimentally and by finite element simulation methods. T wo types of industrially significant steels were selected; they are namely ASTM516-G70, AISI1010 steel; and two shapes of indenters, blunt and sharp (Spherical, and Vickers) were used. The finite element simulation has been performed by the finite element ABAQUS simulation program, and its results were then compared with the experimental test results that extracted from Nanovea instrumented indentation test machine. The results obtained have demonstrated that good agreement between the experimental and the finite element simulation results within 5 % difference for young's module and 7.7 % for yield strength. Whereas excellent agreement is observed at the elastic region and the beginning of the plastic region for engineering stress-strain curve. Finally, it is to be emphasized that the obtained results are more applicable for the tested materials and further research is recommended to accommodate other materials as well and to confirm the generality of this method.

Keywords: finite element simulation; ABAQUS; Instrumented indentation.

1. INTRODUCTION:

An instrumented indentation test or sometimes called depth-sensing indentation instrument test is a test used to obtain mechanical properties such as hardness, Young's modulus, and yield strength by calculation from indenter load-displacement curve. This test can be performed on a microscopic scale. It is partially new and under development to be more flexible and trustworthy in use. The elastic-plastic response of materials to micro indentation is not well understood in either an experimental or theoretical context, nor is there enough experimental information available to support proposed models [3]. Determination of the exact shape of the indenter at the

[*] **Postgraduate Student of Mechanical Engineering at University of Benghazi, Libya**
[*] **Post-Doctoral Follow at University of Waterloo, Waterloo, Ontario Canada Former Lecturer at University of Benghazi, Libya**
[*] **Professor of Mechanical Engineering at University of Benghazi, Libya**

tip is important to the measurement of both hardness and elastic modulus for indentation depths less than a micro scale [4]. Finite element method has been used to simulate conical indentation hardness test. Indentation load-depth curves were obtained, and the elastic modulus was calculated. Results justified and showed that the shapes of the plastic zones depend strongly on both indenter angle and the ratio of young's modulus to yield strength. Where the yield zone of Aluminum $(\frac{E}{\sigma_y} = 157.1)$ is bigger than the yield zone of silicon $(\frac{E}{\sigma_y} = 28.8)$ [5]. Because of the non-linear nature of the Nano-indentation hardness test to obtain the mechanical properties of implanted layers and thin films, the finite element numerical modeling has be attempted and commercial finite code ABAQUS was used. The yield strength, Young's modulus, and hardness of the layer material extracted, with an absolute accuracy of at least 20% [6]. Improving test equipment for instrumented indentation method and consideration to the error sources like error due to pile-up is a way to make it more accurate. Test procedures and concepts are still demanding to improve the method that was introduced before 10 years [7]. Recently, good agreement between experiment Nano indentation hardness test for bulk material and finite element simulation in two-dimensional (2-D) axisymmetric model and a three dimensional (3-D) model have been obtained by using finite element ABAQUS code [9]. Numerical simulations of pure copper, pure titanium, pure iron and copper film are obtained using ABAQUS. It is found that the result depended greatly on mesh size, indenter radius and the hardening law used [10]. Also, a finite element model for spherical indentation test for metallic substrates have been developed and the results was found to be relatively in close agreement to experimental data with very minor effect of Poisson’s ratio on the load displacement curve, but for polymeric materials is less successful because of the effects of anisotropy strain rate dependence e.g., viscosity [11]. Continuous instrumented indentation test with the Oliver–Pharr method using Continuous instrumented indentation test with the Oliver–Pharr method using Vickers's indenter under load values from (10 to 100 N) is performed to determine the mechanical properties of Carbide / aluminum composites. For Vickers hardness numbers, determined by the Oliver–Pharr method and by conventional hardness measurement are found to be in good agreement [12]. Chi Chen (2009), concluded that finite element method (FEM) is an effective tool for simulation of Nano-indentation test on metallic films and limitation caused by simplification of models and

assumptions not be neglected [14]. Abdelbaset Midawi et al. (2016), had found good agreement between yield strength obtained from instrumentation hardness test and yield strength obtained from tensile test for weld zone of X80 pipeline steel [16] . In this study, finite-element method is used to build the indentation model with different indenters geometries in order to understand the contact properties for each indenter shape and to determine the FE indentation load-displacement curves and compare it with the experimental curve to validate the FE model. The advantages and disadvantages of each indenter shape also is discussed, and after model validation the change in friction coefficient, boundary condition and strain hardening exponent to find the effect of these parameters on the load-displacement curve have been investigated. Finally, the validated FE model is utilized to extract mechanical properties and develop the engineering stress-stain curve for selected materials.

2. THEORETICAL BACKGROUND

Nano-indentation hardness test, which is called Instrumented Indentation Hardness, or depth sensing indentation is becoming popular application of contact mechanics used to measure hardness and extract other mechanical properties such as elastic modulus. This is achieved by measuring the indenter penetration ″ h ″ under the applied force P throughout the testing cycle and continue to record the change of the penetration depth after the load removed. The output is called load-displacement curve as shown in (Fig.1), and from it, elastic solution can determine hardness, elasticity modulus, and other mechanical properties [2].

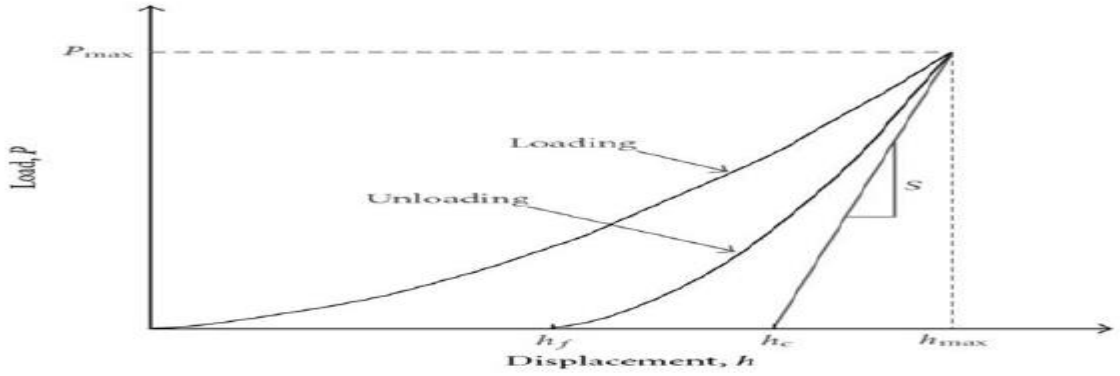

Fig. (1): Load-Displacement curve for indentation test

The hardness can be found by dividing the maximum load on the area of contact or project area, which is determined by depth of the impression and the known angle or radius of the indenter.

$$H = \frac{P_{max}}{A} \qquad (1)$$

The Oliver–Pharr method was originally developed to measure the hardness and elastic modulus of a single-phase elastic-plastic material from the indentation load– displacement curve with sharp indenters, such as Berkovich tip. It has been proven that this method can also be applied in any axisymmetric indenter geometries, including a sphere. As shown in equation (2) the Oliver–Pharr method begins by fitting the unloading portion of the indentation load– displacement data to the power-law relation.

$$P = \alpha\,(h - h_f)^m \qquad (2)$$

Where

α, m are the fitting parameters

h_f Final depth after complete unloading

The slope of the unloaded curve in equation (2) is representing the stiffness, and by using it in equation (4) the Reduced modulus can be found as follows:

$$S = \frac{dp}{dh} \qquad (3)$$

$$S = \frac{2}{\sqrt{\pi}}\, E^* \sqrt{A_p} \qquad (4)$$

Where A_p is the project area.

For spherical indenter according to Multiple-point unloading method the project area equal to:

$$A_p = \pi * a^2 \qquad (5)$$

$$a = \sqrt{2 * R_i * h_p} \qquad (6)$$

Where:

R_i is the indenter radius.

h_p is the plastic penetration depth.

For Vickers indenter the relationship between the projected area A_p of the indentation and the diagonal diameter *d* is:

$$A_p = \frac{d^2}{2\cos 22} = \frac{d^2}{1.845368} \quad (7)$$

$$\frac{dP}{dh} = \frac{d}{\gamma} E^* \sqrt{\frac{2}{\pi}} \quad (8)$$

Where γ is the correction factor equal to 1.0124 for Vickers indenter.

The Reduced modulus and (what is so called) the combined modulus of the indenter and the specimen E^* is given by equation (9).

$$\frac{1}{E^*} = \frac{(1-v^2)}{E} + \frac{(1-\grave{v}^2)}{\grave{E}} \quad (9)$$

Where

$\grave{E}$ $\grave{v}^2$ The elastic modulus and Poisson's ratio of the indenter

E v^2 The elastic modulus and Poisson's ratio specimen

Theoretically, eq. (2) together with eqs. (5) and (7) can be used to find the indentation stress, and by multiplying by *E* the indentation strain can be obtained. Then to extract the stress-strain curve a configuration of the constraint factors, which connect between the normal stress-strain and indentation stress strain as shown [2]:

$$\sigma_{eff} = \frac{\sigma_{ind}}{\psi} \quad (10)$$

$$\varepsilon_{eff} = \beta * \varepsilon_{ind} \quad (11)$$

Where :" ψ " is the stress constraint factor " β " is the train constraint factor.

depends on the material. Generally, the indentation strain constraint factor β is considered to be equal to 0.2, and the indentation stress constraint factor ψ ranges from 2.8 to 3.2 [13].

From the preliminary results of this work, it is found that, the engineering stress-strain converted from the indentation stress- strain curve of a deep spherical indentation test has agreement with effective stress-strain value defined by equations (10) and (11). The stress and strain constraint factor have empirically values according to Taber theory and depended on material properties as shown in Table (1) [15].

Table (1). Constraint factors for different materials [15].

Materials	E (GPa)	n	E/σ_y	ψ	β
Iron	211	0.26	2970.9	3.81	0.141
Steel	210	0.1	420	4.1	0.105
Steell	211	0.12	378.33	4.05	0.11
SUS304	196	0.27	965.517	3.7 3	0.138
Aluminum	70	0.295	5622	3.71	0.131
Al7039OA	71	0.115	265.6	4.05	0.11
Cu-51100	113.69	0.076	256.6	4.11	0.091
Cu-10200	110.24	0.305	3991.31	3.52	0.158
Cu-17510	124.02	0.11	204.26	4.01	0.101
Cu20	110	0.485	25217	3.23	0.131
Cu5.3	125	0.52	28115	3.06	0.152
Au	82	0.25	2050	3.82	0.139
Inconel	170	0.293	646.39	3.8	0.146
A5051	73	0.126	948.05	4.01	0.122
Brass	96	0.36	1633.8	3.51	0.154

3. FINITE ELEMENT SIMULATION

3.1. Reference Materials Considered

As a reference material, AISI 1010 and ASTM 516 G70 were chosen. The mechanical properties for these materials are as shown in Table 2.

The indentation test experiment was performed using the Nanovea mechanical testers, at a maximum load 10N for spherical indentation and 4N for Vickers indentation. The unloading curves were used to derive the modulus values by the analytical technique developed by Oliver and Pharr.

Table (2). Mechanical properties of the reference materials.

Material	Young's modulus E(Gpa)	Yield strength σ_y	Poisson's ratio
AISI 1010	205	220	0.203
ASTM516 G70	240	260	0.23

3.2. Modeling Procedure

In this model, the indentation test of bulk materials with isotropic elastic and plastic properties was simulated by the capability of the ABAQUS finite element (FE) code. Spherical and Vickers rigid indenters are used. A captured view of the models are shown in Fig. (2) and Fig. (3).



Fig. (2): Specimen and indenter tip geometry for spherical indenter in 3D dimension.

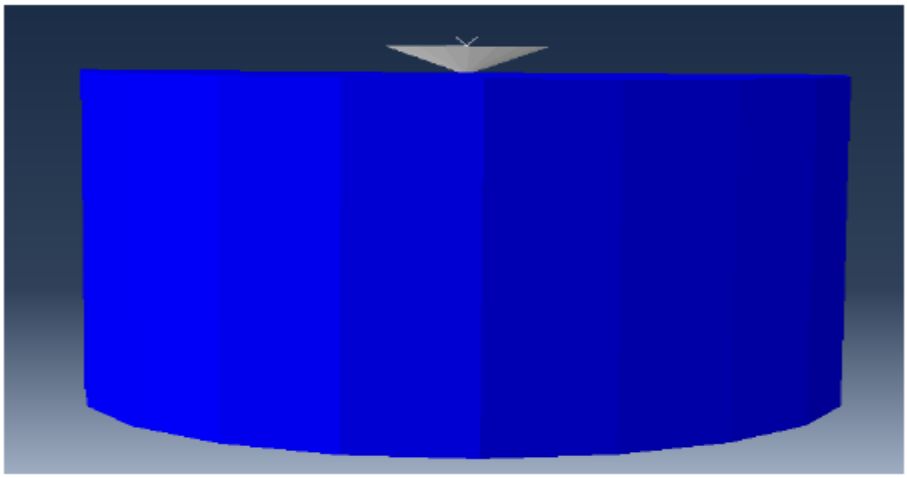

Fig. (3): specimen and indenter tip geometry for Vickers indenter in 3D dimension.

The specimens are modeled with 38416 four-node axisymmetric reduced integration elements (CAX4R element type) for spherical indentation and 43681 for Vickers indentation. A fine mesh is used around the contact area and near the tip of the indenter. The mesh is continuously coarser further away from the tip, as shown in Fig. (4) and Fig. (5).

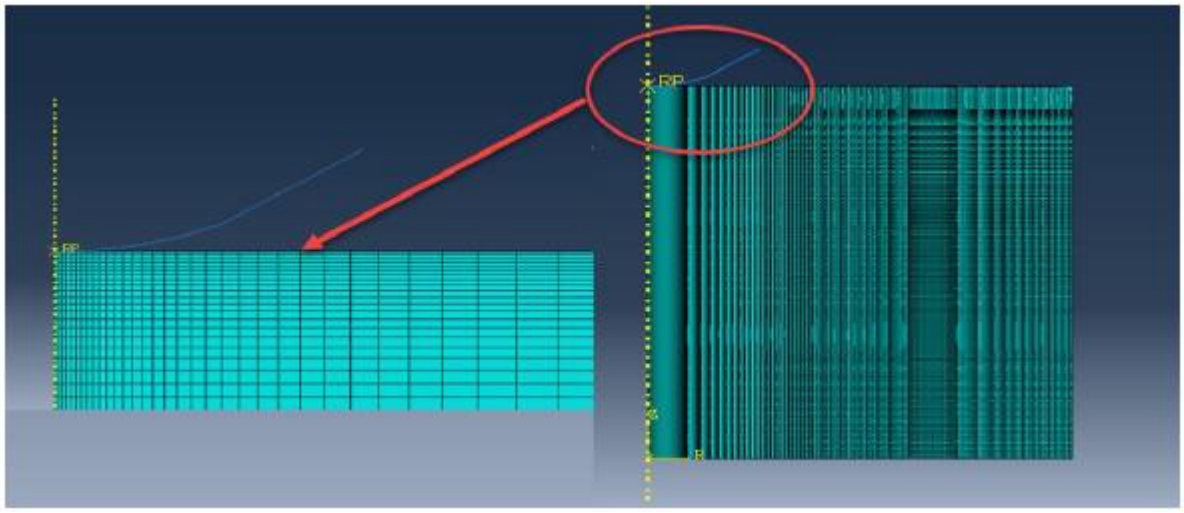

Fig. (4): Meshing density illustration for spherical indentation (38416 elements)

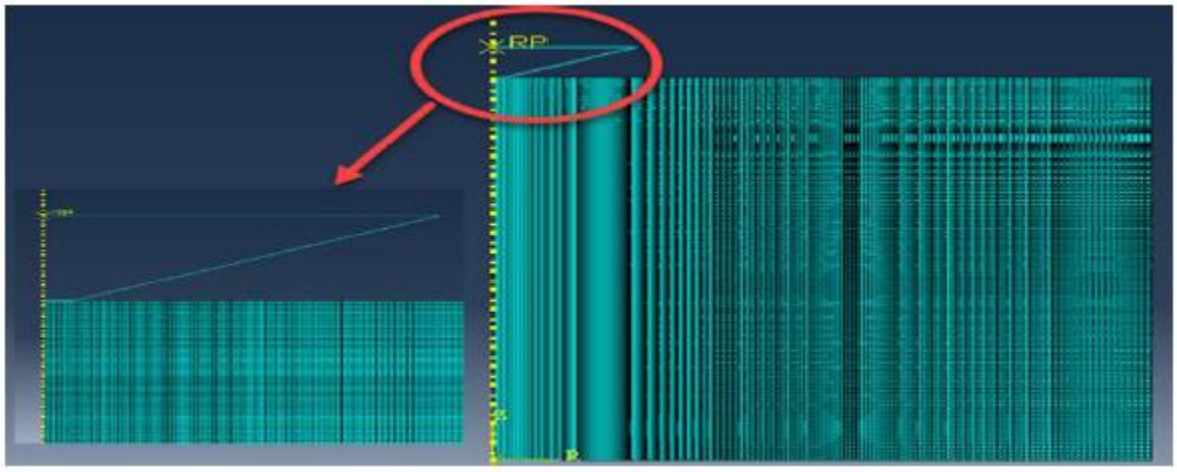

Fig. (5): Meshing density illustration Vickers indentation (43681 elements)

The indentation process is simulated both during the loading and unloading steps. During the loading process the simulation is performed to a depth of 10 μm in the y-direction (U-2) into the specimen; during the unloadi1ng process the indenter tip returns to the initial position as shown in Figs. (6) and (7).

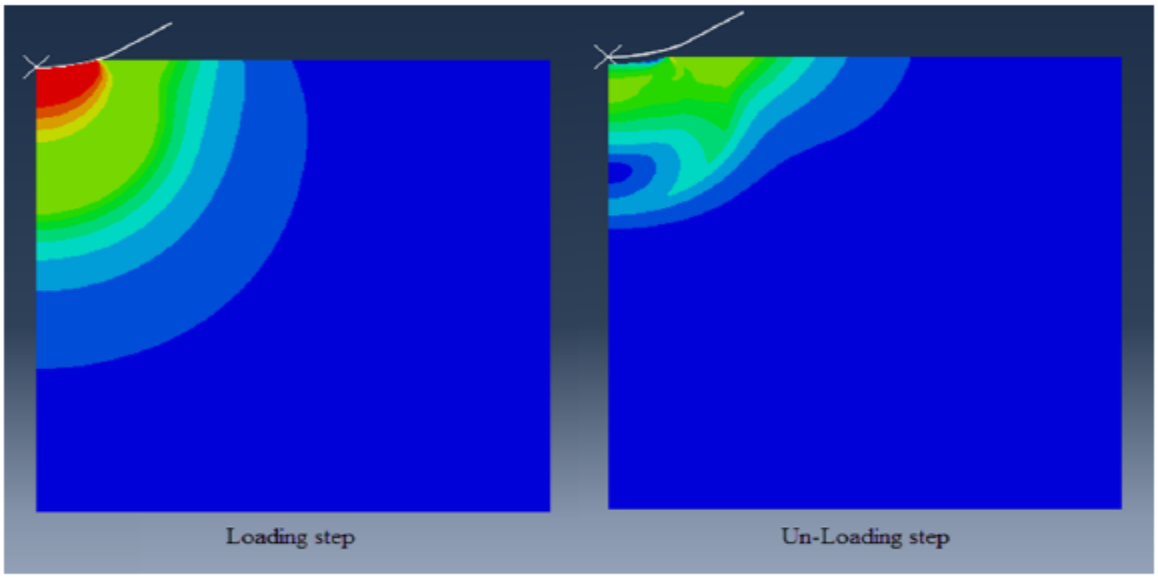

Fig.(6): Loading and Unloading steps for spherical indentation
(Colors represent Stress, Von-Mises)

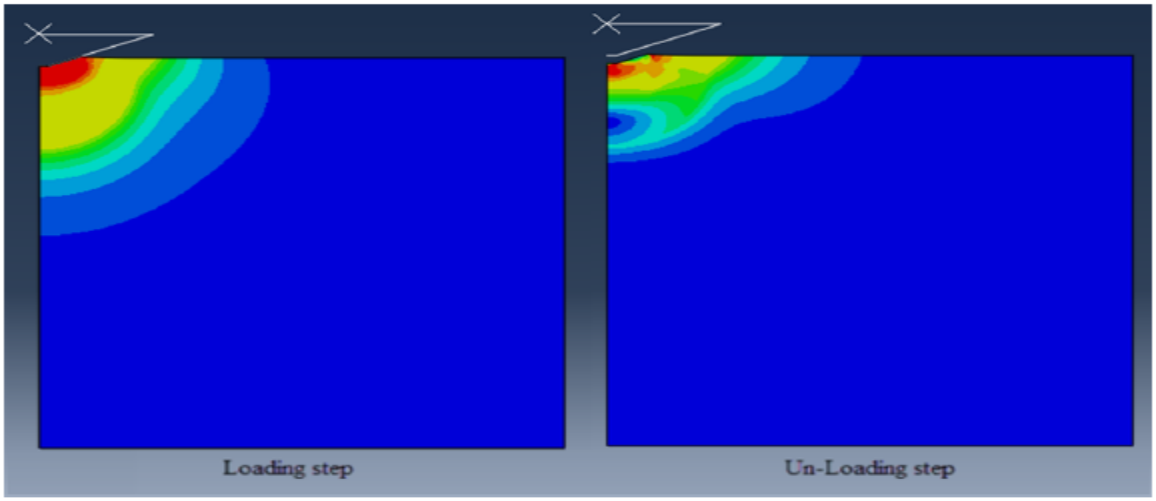

Fig. (7): Loading and Unloading step for Vickers indentation
(Colors represent Stress, Von-Mises)

The contact constraint is defined by the master and the slave surfaces. Because only the master surface can penetrate into the slave surface, the contact direction is then determined by the master surface. The model chooses the indenter as the master surface and the specimen as the slave surface. The boundary conditions are applied along the original point, centerline and bottom of the specimen. The Micro indentation model developed was based on the following assumption:

i. There is perfect interface between the indenter and the substrate so that the indenter and the substrate will not be separated during the indentation process

ii. The friction between the indenter tip and the specimen surface is assumed to be zero.

iii. In the calculation, the elastic deformation occurs in the beginning of the process. The specimen starts to deform plastically when the (σ_{Miss}) reaches to the yield criterion is the yield strength (σ_y).

$$\sigma_{Mises} = \sqrt{\frac{(\sigma_1-\sigma_2)^2+(\sigma_2-\sigma_3)^2+(\sigma_3-\sigma_1)^2}{2}} \qquad (12)$$

Where σ_1, σ_2 and σ_3 are the three principle stresses. There is no strain hardening behavior of the specimen considered in the model

4. RESULTS AND DISCUSSIONS

4.1. Model Validation

To verify the accuracy of the results obtained from FE simulations, Micro-indentation experiments were conducted with a Nanovea mechanical testers. The indenter used for the experiment is the spherical indenter 200 μm diameter and Vickers indenter with 136°. The Two commercial steel grades that widely used in the engineering applications are low carbon steel AISI-1010 and ASTM-516-G70.

Fig. (8) shows comparison between the average experimental curve and simulation load-displacement curve for spherical indenter for AISI1010, and ASTM516G70 materials. As shown excellent agreement between the experimental and the finite element simulation.

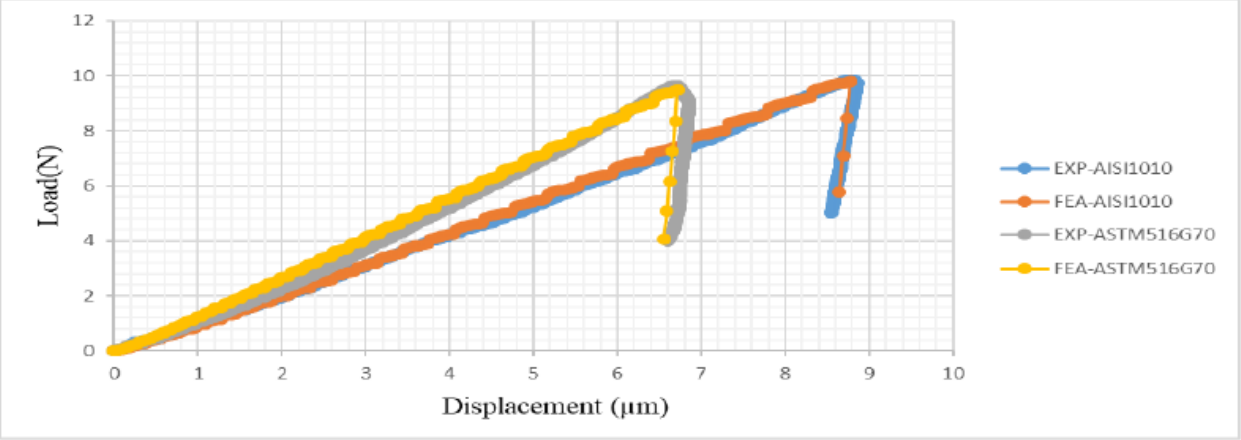

Fig. (8): Comparison of finite element simulation and experimental test results for spherical indenter

Fig. (9) shows comparison between the experimental and simulation load-displacement curves for Vickers indenter. Again, the agreement between results is excellent for both materials (AISI-1010, ASTM-516-G70), which validate the finite element model.

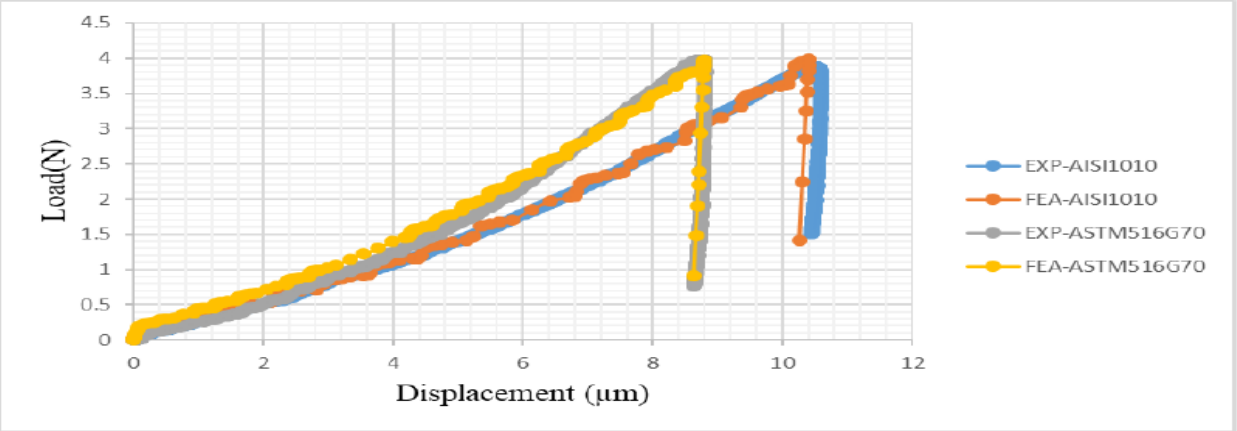

Fig. (9): Comparison of finite element simulation and experimental test results for Vickers indenter

Therefore, based on the above results, the indentation model is validated, and consequently the model can be utilized to extract the stress and strain values for indentation stress-strain curve generation. From this curve and by using eqs. (9) and (10), the engineering stress and strain curve can be generated using suitable constraint factors. This is the same approach which was used by other researchers for other materials as well [16].

4.2. Extracted Engineering Stress-Strain Curve

Figs. (10 & 11) show the FE simulation results for the stress-strain curve, with the experimental curve overlapped on it for spherical indenter. As shown, there is very good agreement between experimental engineering stress-strain curve and the FE simulation stress-strain curve for both materials. Whereas congruence is observed at the elastic region and the beginning of the plastic part as shown. This agreement is considered to be sufficiently enough to estimate the yield stress and the strain hardening exponent as shown in Table (3). The effective stress-strain is obtained by selecting 3.7 to stress constraint factor and 0.11 to strain constraint factor for AISI 1010 and 3.9 and 0.11 for ASTM516-G70. These value are according to published references (Baoxing Xu, 2010) and (Chao Chang, M. A. Garrido ,2018). However, further research work is recommended to be carried out for extending this work to fracture region.

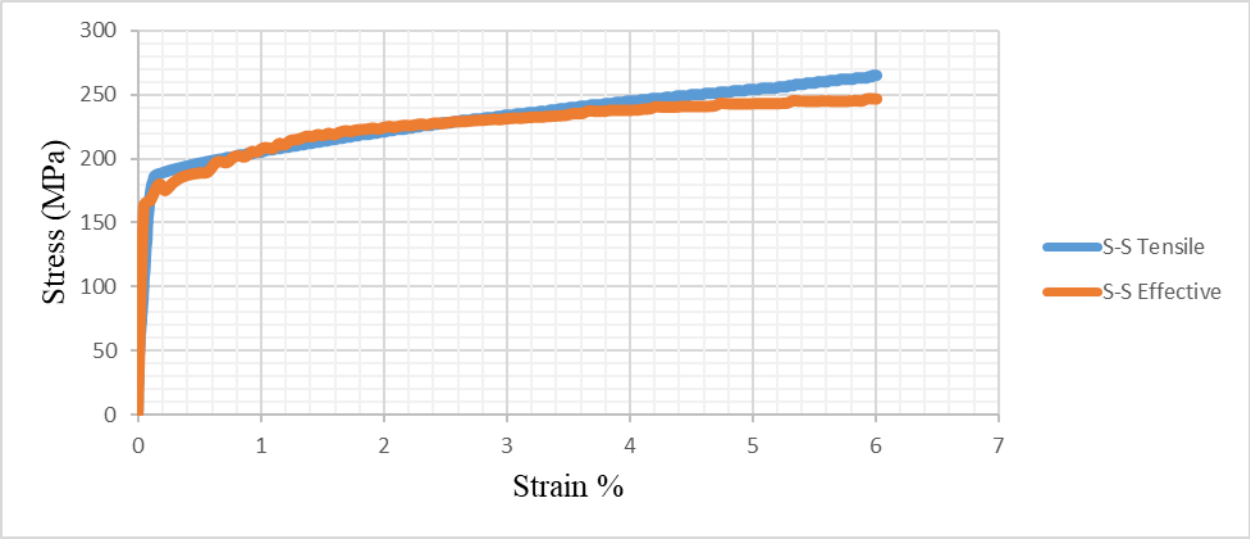

Fig. (10): Comparison between the FE simulation and the experimental engineering stress –strain curves for AISI1010.

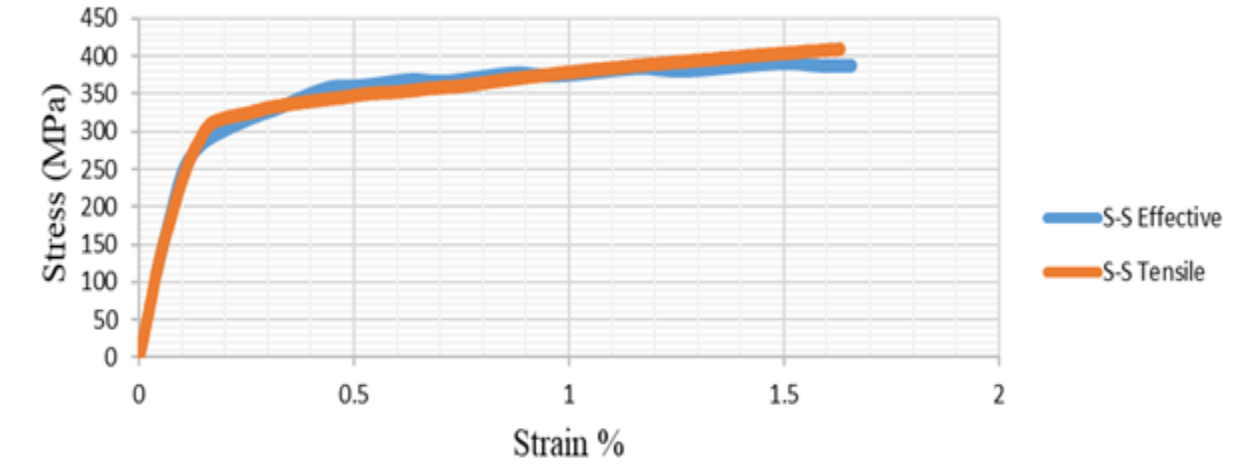

Fig. (11): Comparison between the FE and the experimental Engineering Stress –Strain curves for ASTM516-G70

Table (3). Yield stress and Strain hardening exponent from tensile and FE indentation tests (Spherical indenter)

Material	Yield Stress (Mpa)			Strain hardening exponent			work hardening (Mpa)		
	Tensile test	Indentation test	Error %	Tensile test	Indentation test	Error %	Tensile test	Indentation test	Error %
AISI1010	220	225	2.3	0.149	0.091	38.9	395.51	321.96	18.6
ASTM516-G70	260	280	7.7	0.154	0.139	9.7	315.85	388.25	22.9

4.3. Modulus of Elasticity Prediction

Table (4) compares results for elastic modulus extracted from indentation experimental and finite element simulation methods and also from standard tensile test. As shown a very good agreement obtained from the finite element simulation model as compared with other methods and the error % is within acceptable limits for both materials.

Table (4) Comparison of module of elasticity obtained with different methods for spherical indenter

Material	Modulus of elasticity (GPa)				
	Standard	Tensile test	Indentation test (experimental)	Indentation test (FEM)	Error %
AISI-1010	190-210	203	201.609	203.128	0.06
ASTM-516	200	240	253.44	252	5

5. CONCLUSION

In this research work, the FE method has been implemented using the ABAQUS software to simulate the instrumented indentation test based on the material properties obtained from the

uniaxial tensile tests of ASTM516G70 and AISI1010 steel. From this study the following points have been concluded:

• The FE simulated loading-unloading curves for both ASTM516G70 and AISI1010 steel materials agree well with experimental loading-unloading curves.

• The agreement between the properties obtained from the FE simulation results and experimental mechanical properties is excellent. The results obtained have demonstrated that good agreement between the experimental and the finite element simulation results within 5 % difference for young's module and 7.7 % for yield strength.

• With respect to engineering stress –strain curve, excellent agreement is observed at the elastic region and the beginning of the plastic region. Further research work need to be carried out for extending this work to fracture region.

• Generally, finite element simulation has become a powerful tool to study the micro- indentation test and thus to improve the development in the mathematical theories used to extract mechanical properties from instrumented indentation non-destructive tests.

• Finlay, the FE simulation helps to lower the cost and duration of experimental studies by accurate and fast computational models.

تقييم إختبار الصلادة الحديث كأداة لحساب الخصائص الميكانيكية للمواد الهندسية

الملخص: أصبحت طريقة إختبار الصلادة الحديث من الاختبارات المشهورة في عالم قياس الخصائص الميكانيكية للمواد كالصلادة و معامل المرونة و إجهاد الخضوع كما أصحبت كطريقة لإيجاد منحنى الاجهاد و الانفعال الناتج من إختبار الشد التقليدي كونه يعطي سماحية لقياس الخصائص الميكانيكية للعينات الصغيرة و التى تكون في الموقع و كذلك لكونه إختبار غير هدام .العديد من الابحاث عملت على تقييم هذه الطريقة و معرفة العوامل المؤثرة على نتائجها و بإستخدام أشكال مختلفة من المثالم و أنواع مختلقة من المواد. في هذه الدراسة و لتقييم هذه الطريقة تم إختيار نوعين من حديد الفولاذ هما (ASTM 516G70,AISI 1010) , و بإستخدام شكلين مختلفين من المثالم هما الكروي و المسنن (Spherical , Vickers) حيث إجري تحليل المحاكاة الرقمية بإستخدام طريقة العناصر المتناهية (FEM) بواسطة برنامج الاباكوس (ABAQUS) و مقارنة النتائج المتحصل عليها مع نتائج الاختبار العملي (Experimental) و التي إجريت لهذه المواد تحت نفس الظروف. في هذا البحث ؛ النتائج التي تحصلنا عليها تظهر توافقا بين النتائج المتحصل عليها من الاختبار العملي و النتائج المتحصل عليها من المحاكاة الرقمية حيث أن نسبة الاختلاف في معامل اللدونة كانت لا تتجاوز 5% و 7.7% لإجهاد الخضوع.بألاضافة للخصائص الميكانيكية تم إيجاد منحنى الاجهاد و الانفعال المشابه لمنحنى الاجهاد و الانفعال المتحصل عليه من إختبار الشد عن طريق المحاكاة الرقمية حيث وجد التوافق الكبير في مرحلة التشكيل المرن و بداية مرحلة التشكيل اللدن.كما لوحظ أن طريقة إختبار الصلادة الحديث تعتمد على مجموعة من المعادلات التجريبية أو شبه التحليلية مما يجعل هذا الاختبار محل للتقييم المستمر ليشمل أكبر عدد ممكن من المواد

REFERENCES:

[1] ABAQUS Version 6.14 User's Manual.

[2] D. Tabor, 1951 Hardness of Metals, Clarendon, Oxford, UK.

[3] S. S Chiang D.B. Marshall and A.G. Evans ,1982, The response of solids to elastic plastic indentation, Journal of Applied Physics 53, 298.

[4] M.F. Doerner,1986, A method for interpreting the data from depth-sensing indentation instruments, Journal of Materials Research, Vol 1, Issue 4, pp.601-609.

[5] A.K. Bhargava, C.P. Sharma 1990, Mechanical behavior and testing of materials, PHI Learning Private Limited, Delhi, ISBN -978-81-203-4250-7.

[6] J.A. Knapp,1996, Finite-element modeling of Nano indentation for determining the mechanical properties of implanted layers and thin films, Science Direct, Nuclear Instruments and Methods in Physics Research Section B: Beam Interactions with Materials and Atoms Vols 127–128, PP 935-939.

[7] W.C. Oliver, G.M. Pharr,1992, an improved technique for determining hardness and elastic modulus using load and displacement sensing indentation experiments, Materials Research Society, Vol 7 No 6.

[8] Anthony.C. Fischer-Cripps,2002, Mechanical Engineering Series Nano indentation, Springer Science and Business Media New York, ISBN 978-0-387-22462-6.

[9] Nurot Panich1,2004, Finite Element Simulation of Nano indentation of Bulk Materials, J. Sci. Res. Chula. Univ., Vol. 29, No. 2.

[10] J.D. Bressan, A. Tramontin, C. Rosa,2004, Modeling of Nano indentation of bulk and thin film, Joinville Department of Mechanical Engineering, Universidade do Estado de Santa Catarina (UDESC), 89223-100 Joinville, SC, Brazil.

[11] John D. Clayton,2005, Spherical Indentation in Elastoplastic Materials: Modeling and Simulation, Army Research Laboratory ARL-TR-3516.

[12] Eduard Kimmari and Lembit Kommel ,2006, Application of the continuous indentation test method for the characterization of mechanical properties of B4C/Al composites, Proc. Estonian Acad. Sci. Eng., 12, 4, pp.399–407.

[13] F. Yang and J. C.-M. Li,2008, Micro and Nano Mechanical Testing of Materials and Devices, Springer.

[14] Chi Chen,2009,2-D finite element modeling for Nano indentation and fracture stress, Graduate Theses and Dissertations.http:// scholarcommons.usf.edu/etd/1897

[15] Baoxing Xu, Xi Chen,2010, Determining engineering stress–strain curve directly from the load–depth curve of spherical indentation test, Materials Research Society, J. Mater. Res., Vol. 25, No. 12

[16] Abdelbaset R. H. Midawi, Y. Kisaka, E.B.F. Santos, A.P. Gerlich,2016, Characterization of local mechanical properties of X80 pipeline steel welds using advanced techniques Paper, The American Society of Mechanical Engineers (ASME) No. IPC2016-64238, pp. V003T05A042; 8 page doi:10.1115/IPC2016-64238.